Interaction of Alkanes with Unsaturated Metal Centers. 2. Complexes of Alkanes and Fluoroalkanes with $W(CO)_5$ in the Gas Phase[1]

Carl E. Brown,[2a] Yo-ichi Ishikawa,[2b] Peter A. Hackett,* and David M. Rayner*

Contribution from the Laser Chemistry Group, Division of Chemistry, National Research Council Canada, 100 Sussex Drive, Ottawa, Ontario K1A OR6, Canada. *Received August 23, 1989*

Abstract: Time-resolved infrared spectroscopy has been used to study the interaction of a range of open-chain, cyclic, and fluorine-substituted alkanes with the 16-electron species $W(CO)_5$. $W(CO)_5$ forms reversible complexes with all the unsubstituted alkanes studied except CH_4. The equilibrium constant $K_p = [W(CO)_5L]/([W(CO)_5]p(L))$, at 300 K, increases with carbon number from 610 ± 100 atm^{-1} in ethane to 5200 ± 1600 atm^{-1} in *n*-hexane, and from 1300 ± 400 atm^{-1} in cyclopropane to 7300 ± 2000 atm^{-1} in cyclohexane. Binding energies have also been obtained through temperature studies. They are in the range 7-11 kcal mol^{-1}, again increasing with the size of the alkanes. In the case of CH_4, a binding energy <5 kcal mol^{-1} is implied by our inability to observe a complex. Correlation of the binding energies with C-H σ MO stabilization energies is consistent with a simple molecular orbital picture involving formation of a 2-electron, 3-center C-H-M bond through $\sigma \rightarrow$ M electron donation. Fluorinated alkanes show behavior that depends on the position and degree of substitution. In contrast to CH_4, CH_3F forms a complex with $W(CO)_5$, having a binding energy of ~11 kcal mol^{-1}. CF_4 and CHF_3 do not form observable complexes. CH_3CH_2F forms a complex, bound by ~12 kcal mol^{-1}, but CH_3CF_3 does not. This behavior can again be rationalized in terms of C-H σ MO energy levels.

There has been much recent interest in the chemical activation of the C-H bond through oxidative addition of alkanes to coordinatively unsaturated transition-metal centers. It has been proposed that the initial step in this process is the formation of a complex between the intact alkane and the metal center, involving $\sigma \rightarrow$ M electron donation to form a 2-electron, 3-center C-H-M bond.[3,4] Whether this complex proceeds to oxidative addition or simply redissociates is thought to be determined largely by thermodynamic considerations. This proposal was based on the observation of intramolecular C-H-M bridges in a number of stable, nominally 16 valence electron complexes and on indications that unsaturated metal carbonyls form weak intermolecular complexes with intact alkanes. Molecular complexes bound through π or n electron donation are well-known.[5] The concept of σ donation in intermolecular complexes has recently been confirmed through the observation of dihydrogen complexes.[6] This work also raised the possibility that other σ bonds, such as the C-H bond in saturated hydrocarbons, are potential donors.

Intramolecular C-H-M bridges have been known for some time through NMR and neutron diffraction crystal structure studies.[7] They are found in systems containing nominally unsaturated metal centers with suitable acceptor orbitals. Such bonding, with its consequent ring formation, is referred to as agostic to distinguish it from hydridoalkyl systems. Evidence for the interaction of unsaturated transition-metal carbonyl species, $M(CO)_5$ (M = Cr, Mo, W), with CH_4 in low-temperature matrices is found in shifts in the visible and infrared spectra of $M(CO)_5$ with respect to the spectra observed in rare-gas matrices.[8] In alkane solutions the group 6 pentacarbonyls react with solvents so quickly[9,10] that visible transient absorption spectra of "naked" $M(CO)_5$ species have only been observed on a subpicosecond time scale.[11,12] Recently communicated picosecond time-resolved infrared studies have contested this but still put the time scale of solvation at ~40 ps.[13] Laser flash photolysis of $Cr(CO)_6$ in *n*-hexane produces a visible absorption at ~500 nm,[9] assigned to $Cr(CO)_5(n\text{-}C_6H_{12})$. These observations are consistent with the interaction of a solvent molecule with the vacant coordination site. Photolysis (353 nm) of $Cr(CO)_6$ in perfluoromethylcyclohexane (C_7F_{14}) produces an initial absorption, assigned to $Cr(CO)_5$, with λ_{max} at 620 nm, which is very similar to the λ_{max} in neon matrices of 624 nm, in which the interaction between the $Cr(CO)_5$ and the neon is expected to be extremely weak.[10,14] $Cr(CO)_5$ in C_7F_{14} is reported to react 1000 times more rapidly with CO in C_7F_{14} than in $n\text{-}C_6H_{12}$.[10,14] This is a result of the much stronger interaction of the $Cr(CO)_5$ with $n\text{-}C_6H_{12}$ than with C_7F_{14}.

There is also experimental evidence for $Cr(CO)_5(n\text{-}C_6H_{12})$ as a transient species in solution with time-resolved infrared absorption spectroscopy.[15] UV flash photolysis of $Cr(CO)_6$ in CO-saturated $n\text{-}C_6H_{12}$ produced a visible absorption at λ_{max} = 500 nm and IR CO stretching vibrations at 1960 and 1937 cm^{-1}. The photolysis of $LW(CO)_5$ in *n*-heptane solution, where L = PPh_3, $P(O\text{-}i\text{-}Pr)_3$, or $P(OEt)_3$, leads to absorptions attributable to the cis and trans isomers of $[LW(CO)_4S]$, where S = *n*-heptane, in which the unsaturated fragment $LW(CO)_4$ is said to be "solvated" in *n*-heptane.[16] The authors of ref 16 use the term "token ligand" to describe the solvent molecule that interacts specifically with the otherwise vacant coordination site on the unsaturated metal carbonyl.

Molecular orbital calculations on $Cr(CO)_5(CH_4)$ find an attractive potential for CH_4 approaching $Cr(CO)_5$ to form a linear C-H-Cr bond.[17] Estimates for the strength of the interaction range from ~5 kcal mol^{-1} from the theoretical calculations on

(1) Issued as NRC No. 30997.
(2) (a) NRCC Research Associate, 1987-present. (b) NRCC Research Associate 1986-1988, on leave from The Institute of Physical and Chemical Research, Wako, Saitama 351-01, Japan. Present address: Kyoto Institute of Technology, Matsugaski, Sakyoku, Kyoto 606, Japan.
(3) Crabtree, R. H. *Chem. Rev.* **1985**, *85*, 245-269.
(4) Green, M. L. H.; O'Hare, D. *Pure. Appl. Chem.* **1985**, *57*, 1897-1910.
(5) Mulliken, R. S.; Person, W. B. *Molecular Complexes*; Wiley-Interscience: New York, 1969.
(6) Kubas, G. J. *Acc. Chem. Res.* **1988**, *21*, 120-128.
(7) Brookhart, M.; Green, M. L. H. *J. Organomet. Chem.* **1983**, *250*, 395-408.
(8) Perutz, R. N.; Turner, J. J. *J. Am. Chem. Soc.* **1975**, *97*, 4791-4800.
(9) Welch, J. A.; Peters, K. S.; Vaida, V. *J. Phys. Chem.* **1982**, *86*, 1941-1947.
(10) Bonneau, R.; Kelly, J. M. *J. Am. Chem. Soc.* **1980**, *102*, 1220-1221.
(11) Joly, A. G.; Nelson, K. A. *J. Phys. Chem.* **1989**, *93*, 2876-2878.
(12) Simon, J. D.; Xie, X. J. *J. Phys. Chem.* **1986**, *90*, 6751-6753.
(13) Wang, L.; Zhu, X.; Spears, K. G. *J. Am. Chem. Soc.* **1988**, *110*, 8695-8696.
(14) Kelly, J. M.; Long, C.; Bonneau, R. *J. Phys. Chem.* **1983**, *87*, 3344-3349.
(15) Church, S. P.; Grevels, F.-W.; Hermann, H.; Schaffner, K. *Inorg. Chem.* **1985**, *24*, 418-422.
(16) Dobson, E. R.; Hodges, P. M.; Healy, M. A.; Poliakoff, M.; Turner, J. J.; Firth, S.; Asali, K. J. *J. Am. Chem. Soc.* **1987**, *109*, 4218-4224.
(17) Saillard, J.-Y.; Hoffmann, R. *J. Am. Chem. Soc.* **1984**, *106*, 2006-2026.

0002-7863/90/1512-2530$02.50/0 Published 1990 by the American Chemical Society

$Cr(CO)_5(CH_4)$ to 17–20 kcal mol^{-1} measured by NMR for the intramolecular interaction in $(\eta^3$-allyl)$H(CO)_2(Et_2B(pz)_2)Mo$.[18] Photoacoustic calorimetry has been employed to measure metal–ligand bond strengths in $LCr(CO)_5$ complexes for L = CO, PBu_3, CH_3CN, and THF.[19] A comparison of the Cr–CO bond dissociation energies in the *n*-heptane solution and in the gas phase indicates a 10 kcal mol^{-1} stabilization of $Cr(CO)_5$ through *n*-heptane coordination.

Laser-based time-resolved infrared spectroscopy (TRIS) is proving a powerful new method for the study of organometallic chemistry.[20] Recently, we reported the first observation of an isolated *intermolecular* metal carbonyl alkane complex in the gas phase using this technique.[21] $W(CO)_5(C_2H_6)$ was observed by TRIS following the reaction of $W(CO)_5$ with ethane. $W(CO)_5$ was prepared by the XeCl laser photolysis of $W(CO)_6$. The complex was shown to be in equilibrium with its precursors at room temperature. Its observation shows that direct interaction of a single alkane molecule can indeed explain the spectroscopic and kinetic properties of unsaturated metal carbonyls in alkane-containing condensed phases and, hence, that the participation of an alkane complex in the initial stages of C–H bond activation is certainly feasible.

Currently CO laser-based TRIS does not have the range nor the resolution for us to determine the alkane binding mechanism spectroscopically. To attempt to obtain further insight into the nature of the interaction, we have carried out this study of the interaction of a range of open-chain alkanes, cycloalkanes, and fluorinated alkanes with $W(CO)_5$ in the gas phase.

Experimental Section

Our time-resolved infrared spectrometer has been described in detail elsewhere.[22,23] Briefly, the photolysis source in these experiments was an excimer laser, Lumonics 861-4 (XeCl). The probe laser was an NRC-built, line-tunable (1655–2040 cm^{-1}), liquid nitrogen cooled, CW CO laser, the output of which double passes the 12-cm-long reaction cell almost collinear with the photolysis beam. An Infrared Associates HgCdTe detector/preamplifier combination (300-ns rise time) was employed to monitor transient changes in absorption of the probe laser beam. The output from the detector/preamplifier unit was amplified by a Tektronix differential amplifier, recorded with a Biomation 8100 digitizer, and finally stored in a DEC LSI 11/23 computer. One hundred pulses were averaged for each kinetic trace. Time-resolved difference absorption spectra were constructed in the computer from a series of kinetic runs at different probe wavelengths. Normalization for probe intensity changes between runs was achieved by chopping the CW probe beam at 480 Hz, synchronously triggering the photolysis laser at 10 Hz, and using the fast differential amplifier to record small signal changes at high sensitivity simultaneously with total signal strength. CO laser wavelengths were monitored with an Optical Engineering spectrum analyzer. Excimer laser pulse energies were measured after the cell with a Scientec power meter and were monitored continuously throughout each run, before and after the cell, with beam splitters and photodiodes.

$W(CO)_6$ was obtained from Alfa, degassed by several freeze–pump–thaw cycles with dry ice/methanol, and used without further purification. Mixtures of $W(CO)_6$, argon, and alkane were flowed through the cell in the manner described for $V(CO)_6$.[22] Argon (>99.995% purity, Air Products research grade) was used as supplied. Methane (CP Grade), ethane (CP grade), propane (instrument grade), and tetrafluoromethane (CP grade) were obtained from Linde Specialty Gas Ltd. *n*-Butane (instrument grade), cyclopropane (CP grade), and fluoroform (CP grade) were obtained from Matheson Gas Products, isobutane (CP grade) was from Canada Liquid Air, *n*-pentane (99+%) was from Aldrich Chemical Co., *n*-hexane (reagent grade), cyclopentane (99+%), and cyclohexane (99+%) were from BDH Chemicals. Pentafluoroethane (97–99%), 1,1,1-trifluoroethane (97–99%), methyl fluoride (97–99%), and difluoromethane (97–99%) were obtained from SCM Specialty Chemicals. The alkanes were degassed by several freeze–pump–thaw cycles with liquid nitrogen. Argon and alkane flows were controlled by needle valves. Total gas pressures were monitored with an MKS Baratron capacitance manometer. Partial pressure of $W(CO)_6$ was monitored by the attenuation of the CW CO probe laser beam.

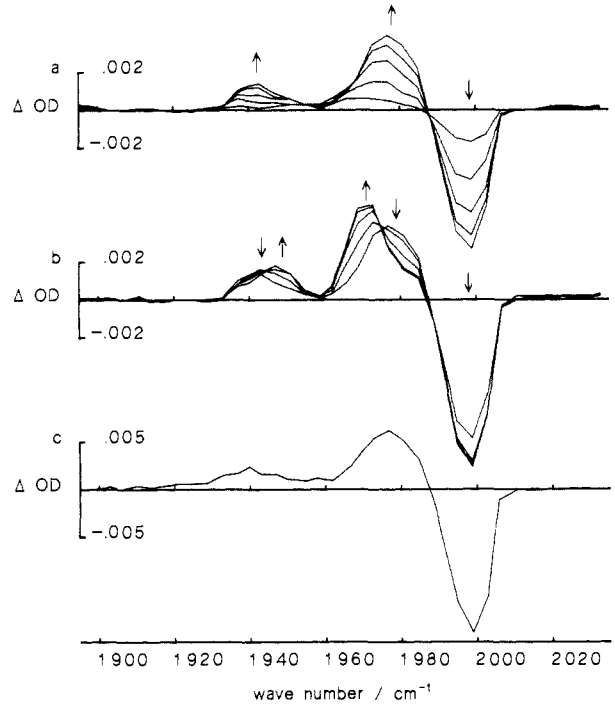

Figure 1. Time-resolved difference absorption spectra (TRIS) following the 308-nm photolysis of a mixture of $W(CO)_6$ and *i*-C_4H_{10} in Ar buffer gas. The pressures of $W(CO)_6$, *i*-C_4H_{10}, and Ar were kept constant at ca. 8 mTorr, 1.09 Torr, and 8.91 Torr, respectively. XeCl laser fluence was ca. 6 mJ cm^{-2}. Early-time spectra (a) were taken at 100-ns intervals over a 0.1–0.5-μs range. Later-time spectra (b) were taken at 500-ns intervals over a 0.5–2.5-μs range. The spectrum in (c) illustrate the absorption due to isolated $W(CO)_5$ at room temperature. An up arrow indicates an increase of ΔOD and a down arrow a decrease.

Results

Previous work in our laboratory has shown that XeCl excimer laser photolysis (308 nm) of gas-phase $W(CO)_6$ produces exclusively the monounsaturated species $W(CO)_5$ at moderate fluences.[24] The photolysis of $W(CO)_6$ in these experiments was therefore performed with an XeCl laser at a few millijoules per centimeter squared fluence. Time-resolved difference absorption spectra of $W(CO)_5$(alkane) complexes were sought following the photolysis of a few millitorr of $W(CO)_6$ in the presence of the alkane and argon buffer gas. Unless otherwise noted, the total pressure was 10 Torr. The dynamics of the systems were studied by observing the kinetic behavior of the transient absorptions at selected infrared wavelengths as a function of constituent gas partial pressures and as a function of temperature.

Open-Chain Alkanes except Methane. In addition to our recently published work on ethane,[21] results have been obtained for the linear alkanes from propane to hexane, for isobutane, and for cyclopropane, -pentane, and -hexane. All showed behavior similar to that of ethane in forming $W(CO)_5L$ complexes in equilibrium in the gas phase. Here we present detailed results on isobutane as representative of the whole class. Figure 1a,b shows the time-resolved difference absorption spectra observed following the 308-nm photolysis (6 mJ cm^{-2}) of $W(CO)_6$ (8 mTorr) in the presence of isobutane (1.09 Torr). In the initial stages (Figure 1a) one can observe the sharpening and blue shifting of the

(18) Cotton, F. A.; Stanislowski, A. G. *J. Am. Chem. Soc.* **1974**, *96*, 5074–5082.
(19) Yang, G. K.; Peters, K. S.; Vaida, V. *Chem. Phys. Lett.* **1986**, *125*, 566–568.
(20) For reviews see: (a) Weitz, E. *J. Phys. Chem.* **1987**, *91*, 3945–3953. (b) Poliakoff, M.; Weitz, E. *Adv. Organomet. Chem.* **1986**, *25*, 277–316.
(21) Ishikawa, Y.; Brown, C. E.; Hackett, P. A.; Rayner, D. M. *Chem. Phys. Lett.* **1988**, *150*, 506–510.
(22) Ishikawa, Y.; Hackett, P. A.; Rayner, D. M. *J. Am. Chem. Soc.* **1987**, *109*, 6644–6650.
(23) Rayner, D. M.; Nazran, A. S.; Drouin, M.; Hackett, P. A. *J. Phys. Chem.* **1986**, *90*, 2882–2888.
(24) Ishikawa, Y.; Hackett, P. A.; Rayner, D. M. *J. Phys. Chem.* **1988**, *92*, 3863–3869.
(25) Koga, N.; Morokuma, K. Abstracts, 35th Symposium on Organometallic Chemistry, Japan, Osaka University, Japan, 1988; pp 25–27.

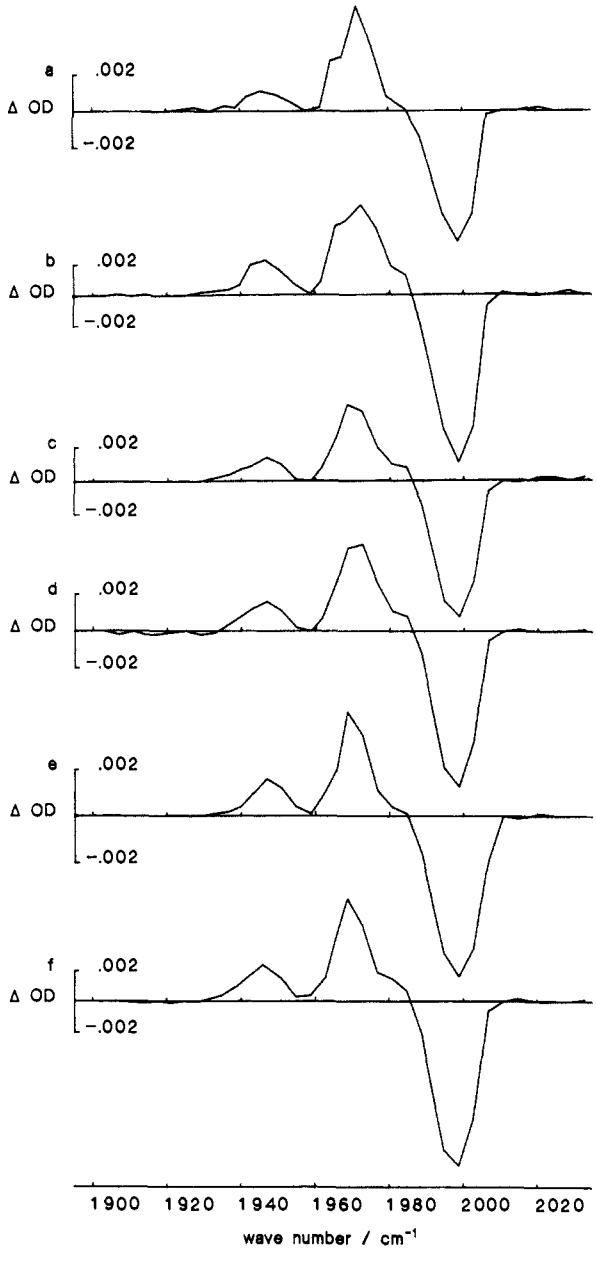

Figure 2. Time-resolved difference absorption spectra (TRIS) of the complexes $W(CO)_5$(alkane) following the 308-nm photolysis of mixtures of $W(CO)_6$ and alkane in Ar buffer gas. $W(CO)_6$ pressure was maintained at ca. 8 mTorr and the total pressure constant at 10 Torr, except for (f) where the total pressure was 5 Torr. The spectra were recorded 3 μs after photolysis. The following pressures of alkane were present in the photolysis mixtures: (a) ethane, 1.39 Torr; (b) propane, 1.37 Torr; (c) *n*-butane, 1.09 Torr; (d) isobutane, 1.09 Torr; (e) *n*-pentane, 0.94 Torr; (f) *n*-hexane, 0.42 Torr.

transient absorptions with time due to the relaxation of the initially internally excited $W(CO)_5$.[24] Figure 1c shows the spectrum of fully relaxed $W(CO)_5$ at room temperature in the gas phase, with absorptions at 1942 (A_1) and 1980 (E) cm^{-1}, respectively.[24] In the presence of isobutane new transient absorptions appear at 1947 and 1973 cm^{-1} shortly after photolysis. The growth of these absorptions is accompanied by the decay of the two $W(CO)_5$ peaks. Isosbestic points are evident at 1945 and 1975 cm^{-1} in Figure 1b. The reaction is complete after ~3–4 μs, and the transient absorption spectrum does not change further over the time span of the experiment (15 μs). We assign the new absorptions at 1947 and 1973 cm^{-1} to the complex $W(CO)_5(i\text{-}C_4H_{10})$. Similar observations were obtained following the photolysis of $W(CO)_6$ in the presence of the other alkanes. The TRIS spectra of the $W(CO)_5L$ complexes, where L = alkane, are illustrated in Figure 2 for the open-chain alkanes and in Figure 3 for the cycloalkanes.

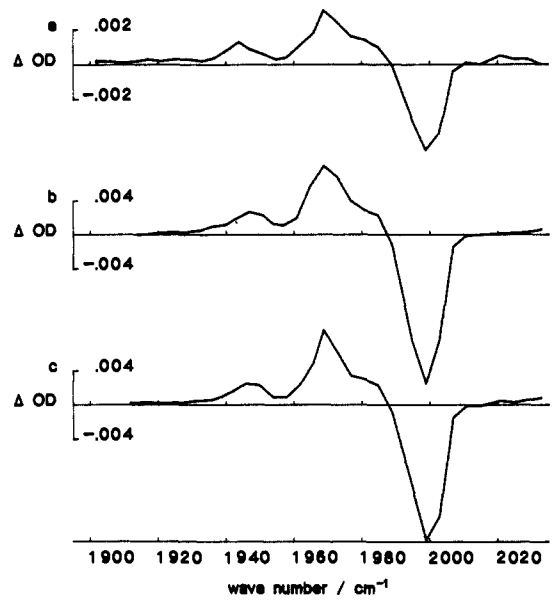

Figure 3. Time-resolved difference absorption spectra (TRIS) of the complexes $W(CO)_5$(cycloalkane) following the 308-nm photolysis of mixtures of $W(CO)_6$ and cycloalkane in Ar buffer gas. $W(CO)_6$ pressure was maintained at ca. 8 mTorr and the total pressure constant at 10 Torr. XeCl laser fluence was ca. 4 mJ cm^{-2}. The spectra were recorded 3 μs after photolysis. The partial pressures of cycloalkane were as follows: (a) cyclopropane, 1.35 Torr; (b) cyclopentane, 0.69 Torr; (c) cyclohexane, 0.49 Torr.

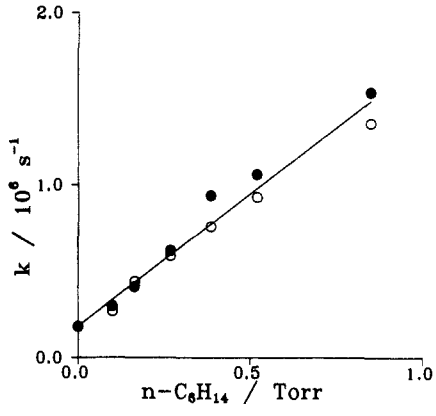

Figure 4. $n\text{-}C_6H_{14}$ pressure dependence of the first-order rate constants for $W(CO)_5$ initial decay (●) and $W(CO)_5(n\text{-}C_6H_{14})$ growth (○). $W(CO)_5L$ and $W(CO)_5$ were monitored at 1969 and 1981 cm^{-1}, respectively, taking spectral overlap into account.

The similarity in the infrared absorption spectrum and the small shifts of the CO stretching band frequencies in the $W(CO)_5L$ complex with respect to those in $W(CO)_5$ suggest that the $W(CO)_5L$ complex retains the overall C_{4v} geometry of $W(CO)_5$.

These assignments are supported by kinetic measurements. As with ethane the $W(CO)_5$ decay and $W(CO)_5L$ growth curves show single-exponential behavior and tend to nonzero asymptotes. Both the rates of these processes and the asymptote levels show a characteristic dependence on the alkane pressure. For ethane[21] this was demonstrated to be due to the establishment of the equilibrium

$$W(CO)_5 + L \underset{k_{-1}}{\overset{k_1}{\rightleftharpoons}} W(CO)_5L \qquad (1)$$

and the same holds for all the saturated alkanes except methane.

Rate constants for the decay of $W(CO)_5$ and the growth of $W(CO)_5L$ were estimated from first-order fits to the latter portion of the transient absorption curves where $W(CO)_5$ relaxation does not interfere. A typical plot of the dependence of the rates of decay of $W(CO)_5$ and the growth of $W(CO)_5L$ on alkane pressure is illustrated in Figure 4, where L = $n\text{-}C_6H_{14}$. The superimposable

Table I. Infrared C-O Stretching Frequencies and Formation Rate Parameters for $W(CO)_5$(Alkane) Complexes

alkane	complex CO str/cm^{-1}	bimolecular rate const/10^6 $Torr^{-1}$ s^{-1}	reactn prob ($k/Z_{collisn}$)
C_2H_6[a]	1971, 1947	0.42 ± 0.20	0.02
C_3H_8	1972, 1947	1.36 ± 0.40	0.08
n-C_4H_{10}	1969, 1946	1.70 ± 0.42	0.11
i-C_4H_{10}	1973, 1947	1.68 ± 0.43	0.10
n-C_5H_{12}	1969, 1946	1.61 ± 0.39	0.10
n-C_6H_{14}	1969, 1946	1.54 ± 0.18	0.10
c-C_3H_6	1969, 1944	0.63 ± 0.24	0.04
c-C_5H_{10}	1969, 1947	0.98 ± 0.20	0.06
c-C_6H_{12}	1969, 1946	1.16 ± 0.15	0.07
CH_3F	1962, 1940	0.77 ± 0.06	0.05
C_2H_5F	1959, 1937	0.99 ± 0.08	0.05
CH_2F_2	1965, 1944	0.20 ± 0.07	0.02
$W(CO)_5$[b]	1980, 1942		

[a] Reference 21. [b] Reference 24.

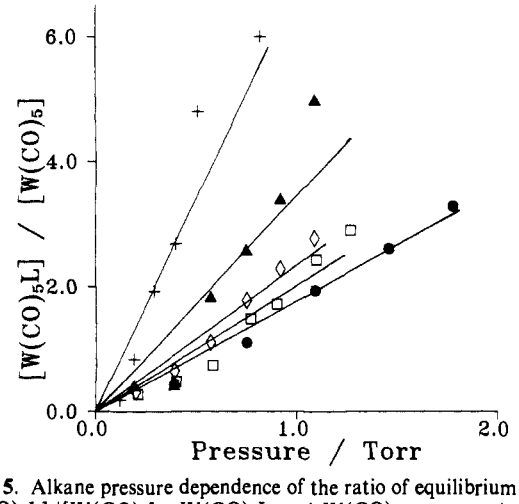

Figure 5. Alkane pressure dependence of the ratio of equilibrium yields, $[W(CO)_5L]/[W(CO)_5]$. $W(CO)_5L$ and $W(CO)_5$ were monitored at 1969 and 1981 cm^{-1}, taking spectral overlap into account: ●, propane; □, n-butane; ◇, isobutane; ▲, n-pentane; +, n-hexane.

straight-line dependence observed for the two processes is expected from the equilibrium (1). With $p(W(CO)_6)$ held low enough so that k_2 for the binucleation reaction

$$W(CO)_5 + W(CO)_6 \xrightarrow{k_2} W_2(CO)_{11} \qquad (2)$$

ensures $k_1p(L) \gg k_2p(W(CO)_6)$, this mechanism requires that $W(CO)_5$ decays and $W(CO)_5L$ grows with the same rate constant, $(k_1p(L) + k_{-1})$. Bimolecular rate constants for the reaction of the alkanes with $W(CO)_5$, along with the associated reaction probabilities, are listed in Table I. The reaction probabilities were calculated with collision diameters estimated from geometrical parameters given in the Appendix.

The rate of dissociation of the complex, k_{-1}, and hence the equilibrium constant, $K_p = k_1/k_{-1}$, is theoretically available from the intercept of plots such as Figure 4. However, there is a large uncertainty in k_{-1}, and K_p is determined better from the asymptote levels of the transient absorption curves. Relative absorption coefficients at the monitoring wavelengths for $W(CO)_5$ and $W(CO)_5L$ were estimated from transient absorption measurements in the absence of alkane and at pressures of alkane where the insensitivity to further added alkane showed the equilibrium to be significantly to the right. Equilibrium ratios, $[W(CO)_5L]/[W(CO)_5]$, at intermediate pressures could then be calculated from the ratio of the asymptote absorption levels. Plots of $[W(CO)_5L]/[W(CO)_5]$ versus pressure of alkane, $p(L)$, showing a linear dependence, passing through zero, are illustrated in Figure 5. The slopes of these plots yield the equilibrium constants at room temperature. The equilibrium constants thus obtained for the various alkanes are listed in Table II.

Table II. Equilibrium Constants, Binding Energies, and Binding Enthalpies for $W(CO)_5$(Alkane) Complexes

alkane	K_p/atm^{-1}	$\Delta E°_0$[a]/kcal mol^{-1} i	ii	iii	$\Delta H°_{300}$[b]/ kcal mol^{-1}	C-H σ MO IP/eV
CH_4					<5	14.33[c]
C_2H_6	610 ± 100	11.9	15.4	9.0	7.4 ± 2[d]	12.35[c]
C_3H_8	1300 ± 400	13.2	16.8	10.2	8.1 ± 2	11.51[c]
n-C_4H_{10}	1500 ± 500	13.5	17.5	10.6	9.1 ± 3	11.66[c]
i-C_4H_{10}	1700 ± 500	12.9	16.8	9.9	8.6 ± 2	11.13[c]
n-C_5H_{12}	2600 ± 800	14.1	18.2	11.2	10.6 ± 3	10.93[c]
n-C_6H_{14}	5200 ± 1600	14.7	19.0	11.7	10.8 ± 3	
c-C_3H_6	1300 ± 400	13.7	17.0	10.8	8.8 ± 2	13.00[e]
c-C_5H_{10}	4600 ± 1400	15.4	19.1	12.5	10.2 ± 3	11.01[e]
c-C_6H_{12}	7300 ± 2000	15.9	19.7	12.8	11.6 ± 3	10.32[e]
CH_3F	3501 ± 1100	13.8	17.3	10.9	11.2 ± 3	13.04[e]
CH_2F_2					>5	13.29[e]
CHF_3					<5	14.80[e]
CF_4					<5	16.23[e]
C_2H_5F	3200 ± 1000	14.2	18.4	11.3	12.2 ± 3	12.43[f]

[a] Binding energies calculated from K_p on the basis of the following models: (i) one vibration at 430 cm^{-1}, four vibrations at 100 cm^{-1}, one free rotation about the W-H-C axis, $\Delta H°_{300} = \Delta E°_0 + 0.3$; (ii) "rigid" complex, $z_i = 1$, $\Delta H°_{300} = \Delta E°_0 + 2.4$; (iii) "loose" complex, five vibrations at 50 cm^{-1}, one free rotation about the W-H-C axis, $\Delta H°_{300} = \Delta E°_0 - 0.6$. [b] Binding enthalpies from van't Hoff plots. [c] Reference 26. [d] This value for $\Delta H°_{300}$ for ethane is a revision of our previously published value. It lies within the error limits placed on the earlier value and its prefered due to improved temperature measurements. [e] Reference 33. [f] Reference 34.

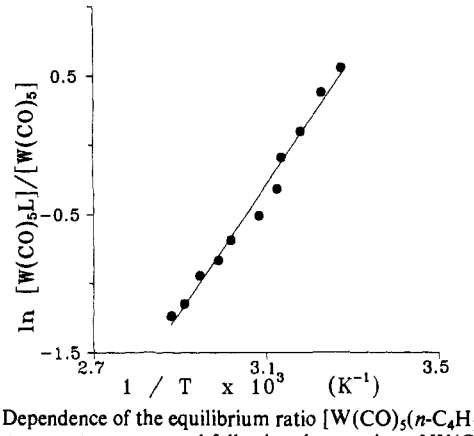

Figure 6. Dependence of the equilibrium ratio $[W(CO)_5(n\text{-}C_4H_{10})]/[W(CO)_5]$ on temperature measured following the reaction of $W(CO)_5$ with n-C_4H_{10}. n-C_4H_{10} pressure was 1.70 Torr and the total pressure 10 Torr (balance Ar).

The final ratio, $[W(CO)_5L]/[W(CO)_5]$, estimated as above, was found to be highly sensitive to temperature. Figure 6 shows a modified van't Hoff plot of ln $([W(CO)_5L]/[W(CO)_5])$ as a function of $1/T$ for L = n-C_4H_{10}. This plot is typical for all of the open-chain alkanes studied except methane. This is the behavior expected of a system in equilibrium, and the slopes lead to values of the binding enthalpy, $\Delta H°_{300}$, for the equilibria. These are listed in Table II.

Binding energies are also accessible through statistical mechanics from the equilibrium constant K_p, measured at a single temperature. On the assumption that the vibrational frequencies of $W(CO)_5$ and the alkane are not changed significantly in the complex, K_p, in terms of the binding energy, $\Delta E°_0$, is reduced to

$$K_p = \frac{(z_r z_t \prod_{i=1}^{6} z_i)_{W(CO)_5L}}{(z_r z_t)_{W(CO)_5}(z_r z_t)_L} e^{\Delta E°_0/RT} \qquad (3)$$

where z_r and z_t are rotational and translational partition functions and z_i are partition functions associated with the six extra internal degrees of freedom of the complex. Table II also lists binding parameters calculated from this method. z_r and z_t were calculated with the geometrical parameters given in the Appendix. z_i were calculated assuming one vibration at 430 cm^{-1} (W-H stretch),

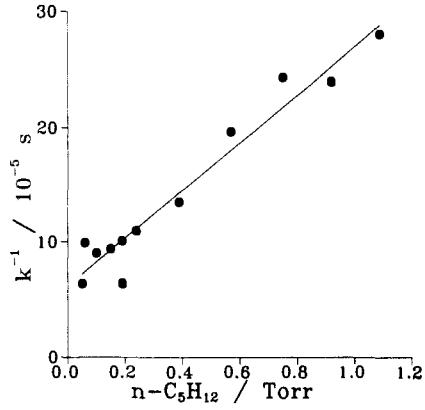

Figure 7. n-C_5H_{12} pressure dependence of the inverse of the first-order rate constant for $W(CO)_5(n\text{-}C_5H_{12})$ decay normalized to 5 mTorr of $W(CO)_6$. $W(CO)_5(n\text{-}C_5H_{12})$ was monitored at 1969 cm^{-1}, taking spectral overlap into account.

four vibrations at 150 cm^{-1}, and one free rotation of the alkane about the W–H–C axis. The values obtained for ΔE°_0 under these circumstances, as well as those obtained if a "rigid" complex is assumed, i.e., $z_i = 1$, and if a "loose" complex with five vibrations at 50 cm^{-1} is assumed, are given. ΔH°_{300} is related to ΔE°_0 through the expression

$$\Delta H^\circ_T = \Delta E^\circ_0 + 4RT - \sum_{i=1}^{6} RT^2\, \mathrm{d}(\ln z_i)/\mathrm{d}T \qquad (4)$$

The adjustments to obtain ΔH°_{300} from ΔE°_0, although model dependent, are small relative to the experimental error in our second law ΔH°_{300} values.

On a longer time scale, $W(CO)_5L$ decays. As shown for L = n-C_5H_{12} in Figure 7, the rate of $W(CO)_5L$ decay was found to increase with decreasing alkane pressure. This is the behavior expected if $W(CO)_5L$ is removed through the loss of its equilibrium partner $W(CO)_5$ rather than its own reaction. In the absence of any alkane, the mechanism for $W(CO)_5$ removal is reaction 2 with the parent carbonyl to form the binuclear complex $W_2(CO)_{11}$.[24] In this case, the rate constant for $W(CO)_5L$ decay is given by $1/k = K_p p(L)/k_2 + 1/k_2$. The straight-line fit in Figure 7 is drawn with K_p for n-C_5H_{12} from the equilibrium yield measurements.

Methane. Methane showed behavior different from that of all the other fully hydrogenated alkanes. TRIS spectra following the photolysis of $W(CO)_6$ in the presence of CH_4 are identical with those found in its absence. We find no evidence for complex formation. This would be consistent with experiments on the gas-phase ultraviolet laser photolysis of $Cr(CO)_6$ where the visible transient absorption spectrum of $Cr(CO)_5$ in CH_4 did not differ from that in He. Experimentally, it is difficult to work at total pressures much greater than ~10 Torr with $W(CO)_6$ in a flowing system. This is due to its low vapor pressure. We were unable to raise the methane pressure or lower the temperature far enough to observe a weaker complex. From our inability to observe a complex under these conditions we put a limit of the CH_4 binding energy at <5 kcal mol^{-1}.

Fluorinated Alkanes. Results were obtained for tetrafluoro-, trifluoro-, difluoro-, and fluoromethane and 1,1,1-trifluoro- and fluoroethane. CF_4, CF_3H, and CH_3CF_3 showed no evidence for reaction with $W(CO)_5$. Time-resolved infrared absorption spectra for the photolysis of $W(CO)_6$ in the presence of CF_4, CF_3H, and CH_3CF_3 are essentially the same as those observed for the photolysis of $W(CO)_6$ in argon alone[24] and are attributed to the formation of the binuclear complex, $W_2(CO)_{11}$, formed by reaction 2.

On the other hand, CH_3F, CH_3CH_2F, and CH_2F_2 reacted with $W(CO)_5$. This is demonstrated by the time-resolved infrared absorption spectra shown in Figure 8. $W(CO)_5(CH_3F)$ has absorption peaks at 1962 and 1937 cm^{-1}, $W(CO)_5(CH_3CH_2F)$ at 1959 and 1935 cm^{-1}, and $W(CO)_5(CH_2F_2)$ at 1965 and ~1944 cm^{-1}. In the case of CH_3F and CH_3CH_2F, the decay of $W(CO)_5$,

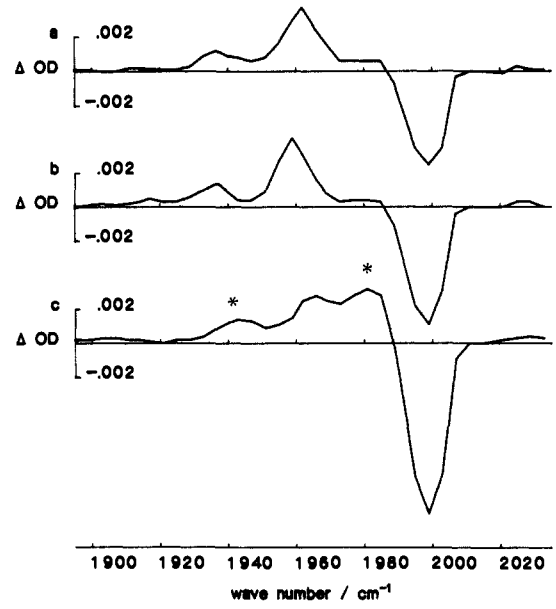

Figure 8. Time-resolved difference absorption spectra (TRIS) of the complexes $W(CO)_5$(fluoroalkane) following the 308-nm photolysis of a mixture of $W(CO)_6$ and fluoroalkane in Ar buffer gas. $W(CO)_6$ pressure was maintained at ca. 8 mTorr and the total pressure constant at 10 Torr. XeCl laser fluence was ca. 4.2 mJ cm^{-2}. The spectra were recorded 3 μs after photolysis. The following pressures of fluoroalkane were present in the photolysis mixtures: (a) methyl fluoride, 1.86 Torr; (b) ethyl fluoride, 1.29 Torr; (c) difluoromethane, 2.87 Torr. The asterisks in (c) indicate the positions of absorptions due to $W(CO)_5$, which is the major component of the photolysis mixture of $W(CO)_6$ and difluoromethane.

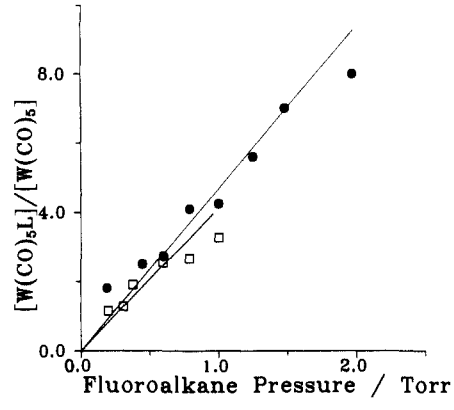

Figure 9. Fluoroalkane pressure dependence of the ratio of equilibrium yields, $[W(CO)_5L]/[W(CO)_5]$. $W(CO)_5L$ and $W(CO)_5$ were monitored at 1959 and 1977 cm^{-1}, taking spectral overlap into account. Key: ●, CH_3F; □, C_2H_5F.

the growth of the fluoroalkane complex peaks, and the asymptotes of the decay curves depended on fluoroalkane pressure in the same manner as observed for the saturated alkanes, showing that these fluoroalkane complexes are at equilibrium at room temperature. Bimolecular rate constants derived from these experiments are given in Table I. Plots of $[W(CO)_5L]/[W(CO)_5]$ for L = CH_3F and CH_3CH_3F are shown in Figure 9, and values of K_p derived from the slopes are given in Table II.

Temperature studies on $[W(CO)_5L]/[W(CO)_5]$ at fixed p(L) were also carried out. The modified van't Hoff plots are shown in Figure 10. Values for the binding enthalpy, ΔH°_{300}, of CH_3F and CH_3CH_2F with $W(CO)_5$ are given in Table II. Again, within experimental error, these values can also be taken as the binding energy.

In the case of CH_2F_2 we were unable to measure a binding energy. The rate of reaction of CH_2F_2 with $W(CO)_5$ is ~5× slower than the other reactive fluoroalkanes. This makes it impossible under our experimental conditions to set up reaction conditions so that the binucleation reaction can be ignored. The

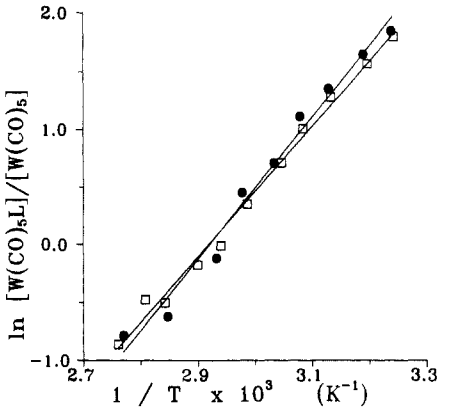

Figure 10. Dependence of the equilibrium ratio $[W(CO)_5L]/[W(CO)_5]$ on temperature measured following the reaction of $W(CO)_5$ with CH_3F (□) and C_2H_5F (●). CH_3F pressure was 2.1 Torr, while the pressure of C_2H_5F was 0.53 Torr. The total pressure in each experiment was maintained at 10 Torr (balance Ar).

problem is exacerbated by overlap between the infrared spectra of $W_2(CO)_{11}$ and $W(CO)_5(CH_2F_2)$. From the fact that a complex is observed in the gas phase, we can put a conservative limit of >5 kcal mol^{-1} on the binding energy in $W(CO)_5(CH_2F_2)$.

Discussion

The $W(CO)_5$(alkane) complexes show infrared spectra that are consistent with the C_{4v} geometry of $W(CO)_5$ being maintained in the complexes. The spectra of all the nonsubstituted alkane complexes are very similar, indicating that the structure and therefore the binding mechanism are the same in all cases. Oxidative addition to form 7-coordinate $W(CO)_5(H)(R)$ species is ruled out by the small shifts to lower frequency observed for the C–O stretching bands. Oxidation of the metal center would result in a shift of these features to significantly higher frequencies outside the range of our CO laser. We observe that the alkane binding energy increases with increasing size. This trend is evident in $\Delta H°_{300}$ measured through the second law, although the error limits associated with these values are relatively large. It is much more clearly reflected in K_p, which increases from 610 ± 100 atm^{-1} in C_2H_6 to 5200 ± 1600 atm^{-1} in n-C_6H_{14} and 7400 ± 2000 atm^{-1} in c-C_6H_{12}. As long as the binding mechanism remains the same, as indicated by the $W(CO)_5L$ TRIS, the preexponential function in the statistical mechanical expression for K_p, eq 3, is expected to drop with increasing alkane size as the rotational and translational partition functions rise far more rapidly for the free alkane than the complex as the size of the alkane is increased. Any increase in K_p, therefore, requires an increase in $\Delta E°_0$, which in turn reflects an increase in $\Delta H°_0$ (eq 4). Because of the exponential nature of the relationship, small changes in $\Delta E°_0$ are magnified outside the error in K_p. With the proviso that the structure of the complex does not vary, K_p is a sensitive probe of the strength of the interaction.

Figure 11 shows a molecular orbital diagram for the interaction of a C–H bond with $W(CO)_5$, adapted from Hoffmann's picture for CH_4 binding to $Cr(CO)_5$. Like $Cr(CO)_5$, C_{4v} $W(CO)_5$ has an unoccupied a_1 MO lying above a fully occupied set of t_{2g} MOs. In an approach where C–H–M are collinear, a weakly bonding orbital is formed through interaction of the C–H σ MO with the a_1 MO. A binding energy of 5 kcal mol^{-1} was estimated for $Cr(CO)_5(CH_4)$. In C–H, unlike H–H where M → σ^* donation results in significant stabilization, side-on bonding is not thought to be favored. This is due to a repulsive interaction between the C–H σ MO and two of the t_{2g} set of MOs, which negates any stabilization arising from a binding interaction between the t_{2g} MOs and σ^* on the C–H.

In the above σ → M model the strength of the interaction is expected to depend on the level of the C–H σ MO. Stronger bonding is expected if the level of this MO is raised to match that of the metal a_1 MO more closely. Photoelectron spectroscopy supported by ab initio calculations shows that the C–H σ MO

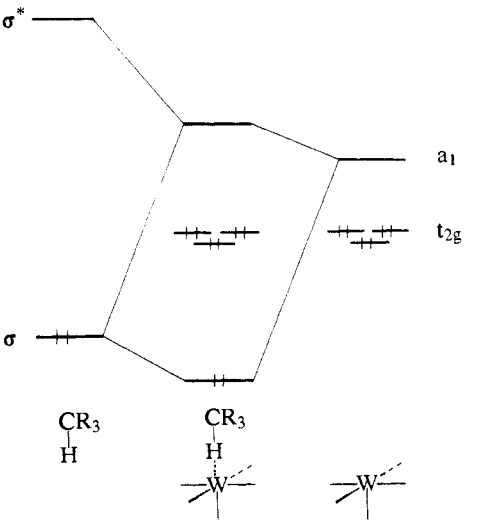

Figure 11. Interaction diagram for the perpendicular approach of a C–H bond to $W(CO)_5$.

in alkanes rises with increasing alkane size.[26] C–H σ MO ionization energies are compared with our alkane binding energies in Table II. The largest change in MO stabilization energy is in the interval between CH_4 and C_2H_6 where the largest change in alkane binding energy (from <5 to 7.4 kcal mol^{-1}) is observed. The correlation between the binding energy and the level of the C–H σ MO is as expected for a σ → M bonding mechanism. Whether another binding geometry could also be consistent with these results is open to question. The possibility of a bifurcate structure in which two C–H bonds interact with the tungsten center cannot be ruled out. Recent ab inito molecular orbital calculations point to such a structure for the model C–H activation intermediate $(CH_4)RhCl(PH_3)_2$.[25] In this system both donation and back-donation are proposed to take place, and the effect the C–H σ MO level would have on such binding in the $W(CO)_5L$ system is not easily predicted. There are no trends in our data that point to preferential binding by primary, secondary, or tertiary C–H bonds. For instance, n-C_4H_{10} and i-C_4H_{10} have the same binding energy within error, as do C_3H_8 and c-C_3H_6.

Substitution of fluorine atoms into the alkanes is a probe of the binding mechanism as long as alkyl C–F bonds cannot interact with $W(CO)_5$ through a mechanism of their own. UV/visible flash photolysis studies of $Cr(CO)_6$ in perfluorinated solvents indicate that there is little or no interaction between the C–F bond or the F lone pairs and $Cr(CO)_5$. We found no evidence for complex formation between $W(CO)_5$ and CF_4 in these TRIS studies. With the caveat that a weakly attractive C–F–M interaction has recently been proposed in intramolecular arylfluorocarbon complexes,[27,28] it is therefore unlikely that complex formation in partially fluorinated alkanes is due to a different form of bonding involving the fluorine atoms directly. The binding properties of fluorinated alkanes to $W(CO)_5$ are shown in Table II. At first it is perhaps surprising that this class of compounds can form complexes at all. The inductive effect of a highly electronegative fluorine atom might be expected to reduce the ability of any such substituted alkane to act as an electron donor. This is clearly not the case. However, the selective binding, which is dependent on the position and degree of fluorination, can be rationalized on the basis of 3-center bond formation through C–H σ M donation. Photoelectron spectroscopy shows a significant destabilization of the C–H σ MOs in CH_3F, CH_2F_2, and CH_3CH_2F compared to CH_4,

(26) Kimura, K.; Katsumata, S.; Achiba, Y.; Yamazaki, T.; Iwata, S. *Handbook of HeI Photoelectron Spectra of Fundamental Organic Molecules*; Halstead Press: New York, 1981.

(27) Uson, R.; Forniés, J.; Tomás, M.; Cotton, F. A.; Falvello, L. R. *J. Am. Chem. Soc.* **1984**, *106*, 2482–2483.

(28) Kulawiec, R. J.; Holt, E. M.; Lavin, M.; Crabtree, R. H. *Inorg. Chem.* **1987**, *26*, 2559–2561.

and it is these molecules that form complexes while CH_3CF_3 and CHF_3 do not.

The ability to form a C–H–M bond might also be predicted from the charge density on the hydrogen atom in the alkane, the more negative charge on the hydrogen favoring bonding. Charge density calculations in these systems are notoriously dependent on the choice of basis set; however, it is interesting to note that ab initio calculations on fluoroalkanes have predicted the sign of the charge to alternate from negative on hydrogens α to fluorine to positive on β-hydrogens.[29] The fact that we observe binding in CH_3CH_2F but not in CH_3CF_3 is consistent with these calculations and the formation of a 3-center bond.

Although the evidence from correlations between the C–H σ MO stabilization energy and binding energy points to 3-center bond formation in both saturated and fluorinated alkane complexes, there are differences between the two systems. The time-resolved infrared spectra of the fluorinated alkane complexes, although still consistent with a C_{4v} geometry, are shifted by ~ 10 cm^{-1} to the red compared to the saturated alkane complexes. This shift cannot be linked to increased electron density on the metal, associated with an increased binding energy in the fluorinated alkanes, as the larger saturated alkanes have comparable binding energies but show only very small red shifts in their spectra. The difference is probably due to through space interaction between the fluorine atom(s) and the CO ligands. Monofluorinated alkanes also form stronger complexes than saturated alkanes having comparable C–H σ MO stabilization energies. It is not surprising that the binding cannot be explained fully by a unified model with a single variable, which does not take into account factors, such as overlap, which may differ significantly between the two classes of molecule.

Conclusions

Alkanes, except methane, form intermolecular complexes with the 16-electron species $W(CO)_5$. The binding is weak and is consistent with the formation of a 2-electron, 3-center C–H–M bond through $\sigma \rightarrow$ M electron donation. Consistent with steric inhibition of M $\rightarrow \sigma^*$ back-donation, binding is weaker than in H_2 complexes, the other known σ intermolecular complexes. $W(CO)_5$ is not expected to be a chemical activation system; however, our results indicate the extent to which initial molecular complex formation can contribute to lowering the barrier to oxidative addition.

Appendix

The following collision diameters, σ, were used in the calculation of reaction probabilities listed in Table I (pm): 750 for $W(CO)_5$; 444.3 for C_2H_6; 511.8 for C_3H_8; 468.7 for n-C_4H_{10}; 527.8 for i-C_4H_{10}; 594.9 for n-C_6H_{14}; 480.7 for c-C_3H_6; 618.2 for c-C_6H_{12}.[30] The collision diameters (pm) of the following compounds were estimated to be as follows: 579 for n-C_5H_{12}; 549 for c-C_5H_{10}; 398 for CH_3F; 421 for CH_2F_2; 465 for C_2H_5F.

The rotational (z_r) and translational (z_t) partition functions used in the statistical mechanical calculation of binding energies of the various alkanes to $W(CO)_5$ were calculated with the following geometrical parameters. For all open-chain alkanes except isobutane, the bond lengths and bond angles were as follows: r(C–H), 109 pm; r(C=O), 115 pm;[31] r(W–C), 206 pm;[31] r(W–H), 170 pm; r(C–C), 152 pm; θ(C–C–C), 109.4°; θ_a(C–W–C), 90°; θ_b-(C–W–C), 180°; θ(W–H–C), 180°. In the case of isobutane the following values[32] were used: r(C–H), 111.3 pm; r(C–C), 153.5 pm; $r(C–H)_{tert}$, 112.2 pm; θ(C–C–C), 110.8°; θ(H–C–C)CH_3, 111.4°; $\theta(H–C–C)_{tert-H}$, 108.1°; θ(H–C–H), 107.6°. In CH_3F and C_2H_5F r(C–H) was maintained at 109 pm, r(C–F) set to 134 pm, and all fluoroalkane bond angles were arbitrarily set to 109.4°. The cyclic compounds were approximated to simple planar geometries. The bond lengths and angles employed in the calculations were r(C–H) = 109 pm, r(C–C) = 155 pm, and θ(C–C–C) = 60°, 108°, and 120°, respectively, for cyclopropane, cyclopentane, and cyclohexane.

Registry No. C_2H_6, 74-84-0; C_3H_8, 74-98-6; n-C_4H_{10}, 106-97-8; i-C_4H_{10}, 75-28-5; n-C_5H_{12}, 109-66-0; n-C_6H_{14}, 110-54-3; c-C_3H_6, 75-19-4; c-C_5H_{10}, 287-92-3; c-C_6H_{12}, 110-82-7; CH_3F, 593-53-3; CH_2F_2, 75-10-5; CHF_3, 75-46-7; CF_4, 75-73-0; C_2H_5F, 353-36-6; CH_4, 74-82-8; $W(CO)_5$, 30395-19-8.

(29) Hehre, W. J.; Pople, J. A. *J. Am. Chem. Soc.* **1970**, *92*, 2191–2197.

(30) Reid, R. C.; Prausnitz, J. M.; Sherwood, T. K. *The Properities of Gases and Liquids*; McGraw-Hill: New York, 1976.

(31) Luckehart, C. M. *Fundamental Transition Metal Organometallic Chemistry*; Brooks-Cole: Monterey, 1985.

(32) Chen, S. S.; Wilhoit, R. C.; Zwolinski, B. J. *J. Phys. Chem. Ref. Data* **1975**, *4*, 859–869.

(33) Potts, A. W.; Lempka, H. J.; Streets, D. G.; Price, W. C. *Philos. Trans. R. Soc. London A* **1970**, *268*, 59–76.

(34) Sauvageau, P.; Doucet, J.; Gilbert, R.; Sandorfy, C. *J. Chem. Phys.* **1974**, *61*, 391–395.